Advanced Engineering Forum *Online: 2012-06-04*
ISSN: 2234-991X, Vol. 4, pp 243-248
doi:10.4028/www.scientific.net/AEF.4.243

Acoustic Pressure Minimization for Diffuse Fields

Wen-Kung Tseng

Graduate Institute of Vehicle Engineering,
National Changhua University of Education
Changhua City, Taiwan, R.O.C.

e-mail:andy007@cc.ncue.edu.tw

Keywords: diffuse fields, acoustic pressure minimization, ∞-norm, two-channel, three-channel, secondary sources.

Abstract. In this paper performance of actively controlling diffuse fields using acoustic pressure minimization has been presented. The technique is ∞-norm acoustic pressure minimization. The theory and simulations of pressure minimization over space and frequency using two-channel and three-channel systems are presented. This paper focuses on diffuse primary fields with two and three secondary sources. A constrained pressure minimization is also introduced in this paper, to control pressure at various spaces and frequencies. The results show that a good attenuation is achieved at the microphone location or desired range over space and frequency using a two-channel system and a three-channel system. Also the shape of the attenuation contour could be controlled using the proposed method in this paper.

Introduction

Previous work on active control of diffuse fields investigated the performance of pressure attenuation for single-tone diffuse field only which was produced by single frequency [1, 2]. Recent work on broad-band diffuse fields only concentrated on analysis of auto-correlation and cross-correlation of sound pressure [3, 4]. However there is no paper related to active control of broad-band diffuse fields. Therefore this paper will analyze the sound field and investigate the performance of active control of broadband diffuse fields.

The minimization of acoustic pressure over space and frequency is desirable for achieving a good performance [3], e.g. high attenuation of the broad-band disturbance over a large space. Previous works on active control of broadband disturbance over space and frequency only concerned with a plane wave primary field [3]. However the work presented in this paper concerns with broad-band diffuse primary fields. Moreover a constrained minimization of acoustic pressure is introduced, to achieve a better control of acoustic pressure in both frequency and space. The paper is organized as follows. First, the mathematical model of broad-band diffuse fields is derived. Second, the control method for broad-band diffuse fields is introduced. Then, simulation results of actively controlling broad-band diffuse fields are presented. Finally the conclusions are made.

The wave model of broad-band diffuse fields

Previous work used the wave model for a pure tone diffuse field, which is comprised of large number of propagating waves arriving from various directions [5, 6]. In our study we chose 72 such incident plane waves together with random amplitudes and phases to generate an approximation of a diffuse sound field in order to coincide with that in previous work. Thus the diffuse sound field was generated by adding together the contributions of 12 plane waves in the azimuthal directions (corresponding to azimuthal angles $\varphi_L = L \times 30^0$, L=1,2,3, . . . , 12) for each of six vertical incident directions (corresponding to vertical angles $\theta_K = K \times 30^0$ for K = 1, 2, 3, . . . , 6). The net pressure in the point (x_0,y_0) on the x-y plane due to the superposition of these 72 plane waves was then calculated from the expression

$$P_p(x_0,y_0,k) = \sum_{K=1}^{K\max} \sum_{L=1}^{L\max} (a_{KL} + jb_{KL}) \sin\theta_K \exp(jk(x_0 \sin\theta_K \cos\varphi_L + y_0 \sin\theta_K \sin\varphi_L)) \quad (1)$$

in which both the real and imaginary parts of the complex pressure are randomly distributed. The values of a_{KL} and b_{KL} are chosen from a random population with Gaussian distribution N(0,1) and the multiplicative factor $\sin\theta_K$ is included to ensure that, on average, the energy associated with the incident waves was uniform from all directions. Each set of 12 azimuthal plane waves arriving from a different vertical direction θ_K, is distributed over a length of $2\pi r \sin\theta_K$, which is the circumference of the sphere defined by (r, φ, θ) for θ_K. This results in higher density of waves for smaller θ_K, and thus more energy associated with small θ_K. To ensure uniform energy distribution, the amplitude of the waves is multiplied by $\sin\theta_K$, thus making the waves coming from the ''dense'' direction, lower in amplitude. Substituting $k=\frac{2\pi}{c}f$ into Eq. 1 gives

$$P_p(x_0, y_0, f) = \sum_{K=1}^{K_{max}} \sum_{L=1}^{L_{max}} (a_{KL} + jb_{KL}) \sin\theta_K \exp(j\frac{2\pi}{c} f (x_0 \sin\theta_K \cos\varphi_L + y_0 \sin\theta_K \sin\varphi_L)), \quad (2)$$

Where f is frequency and c the speed of sound. Eq. 2 is the wave model of the pure tone diffuse field since only the single frequency plane wave arriving from uniformly distributed directions is considered. If the diffuse field is broad-band within the frequency range of fl and fh, then the wave model of the broad-band diffuse field $\boldsymbol{P_{pb}}$ can be expressed as

$$P_{pb}(x_0, y_0, fl - fh) = \sum_{f=fl}^{fh} \sum_{K=1}^{K\max} \sum_{L=1}^{L\max} (a_{KL} + jb_{KL}) \sin\theta_K \exp(j\frac{2\pi}{c} f (x_0 \sin\theta_K \cos\varphi_L + y_0 \sin\theta_K \sin\varphi_L)) \quad (3)$$

where *fl-fh* is the frequency range from ***fl*** to ***fh*** Hz. Eq. 3 will be used for broad-band diffuse primary sound field in this work. Next we will describe the formulation of the control method, and their use in the design of broad-band diffuse field quiet zones.

Control method of broad-band diffuse fields

In this section the control method of broad-band diffuse fields is presented. The basic idea is to use ∞ norm pressure minimization over space and frequency for broad-band diffuse fields. In this work, the case of a one-dimensional space and a broad-band diffuse primary field derived in Eq. 3 is considered and the secondary sources are located at the origin and (-0.1m, 0) point. A microphone can be placed at the desired zone of quiet or other locations close to secondary monopoles. The secondary sources are driven by feedback controllers connected to the microphone. The microphone detects the signal of the primary field, which is then filtered through the controllers to drive the secondary sources. The signals from the secondary sources are then used to attenuate the primary disturbance at the pressure minimization region.

The feedback system used in this work is configured using the internal model control [7] as shown in Fig. 1 where P_1 is plant 1, the response between the input to the first monopole and the output of the microphone, P_{1o} is the internal model of plant 1, P_2 is plant 2, the response between the input to the second monopole and the output of the microphone, P_{2o} is the internal model of plant 2, P_{s1} and P_{s2} are the secondary fields at the field point away from the first and second monopoles respectively, d is the disturbance, the broad-band diffuse field, at the microphone location, d_s is the disturbance at the field point away from the microphone, and e is the error signal. In this work, P_{1o} is assumed to be equal to P_1 and P_{2o} is equal to P_2. Therefore the feedback system turns to a feedforward system with $x=d$, where x is the input to the control filters W_1 and W_2. .

The secondary fields at the field point away from the secondary monopoles could be written as:

$$P_{s1}(r_1, f) = \frac{A_1}{r_1} e^{-j2\pi f r_1 / c}, \quad (4)$$

$$P_{s2}(r_2, f) = \frac{A_2}{r_2} e^{-j2\pi f r_2 / c}, \quad (5)$$

where r_1 and r_2 are the distances from the field point to the first and second monopoles, respectively, A_1 and A_2 are the amplitude constants, f is the frequency and c is the speed of sound.

The plant responses can be written as:

$$P_1(r_{1o}, f) = \frac{A_{1o}}{r_{1o}} e^{-j2\pi f r_{1o}/c}, \tag{6}$$

$$P_2(r_{2o}, f) = \frac{A_{2o}}{r_{2o}} e^{-j2\pi f r_{2o}/c}, \tag{7}$$

where r_{1o} and r_{2o} are the distances from the microphone to the first and second monopoles, A_{1o} and A_{2o} are the amplitude constants.

The error signal could be expressed as:

$$\begin{aligned} e_s &= d_s - d_s W_1 P_{s1} - d_s W_2 P_{s2} \\ &= d_s (1 - W_1 P_{s1} - W_2 P_{s2}) \\ &= d_s S. \end{aligned} \tag{8}$$

The term S is the sensitivity function, i.e. $S = (1 - W_1 \frac{A_1}{r_1} e^{-j2\pi f r_1/c} - W_2 \frac{A_2}{r_2} e^{-j2\pi f r_2/c})$.

The disturbance in this work is the broad-band diffuse field, therefore Eq. 8 can also be expressed as:

$$e_s = P_{pb} S \tag{9}$$

Where P_{pb} is the broad-band diffuse primary field as shown in Eq. 3.

The formulation of the cost function to be minimized can be written as.

$$J_\infty = \left\| \sqrt{SP_{pb}} S \right\|_\infty, \tag{10}$$

where $\sqrt{SP_{pb}}$ is the square root of the power spectral density of broad-band disturbance pressure at the field points.

For a robust stability, the closed-loop of the feedback system must satisfy the following condition.

$$\left\| W_1 B_1 \frac{A_{1o}}{r_{1o}} e^{-j2\pi f r_{1o}/c} + W_2 B_2 \frac{A_{2o}}{r_{2o}} e^{-j2\pi f r_{2o}/c} \right\|_\infty < 1, \tag{11}$$

where B_1 and B_2 are the multiplicative plant uncertainty bounds for plants 1 and 2 and r_{1o} and r_{2o} are the distances from the microphone to the first and second monopoles, respectively. The terms $e^{-j2\pi f r_{1o}/c}$ and $e^{-j2\pi f r_{2o}/c}$, that is the plant responses, therefore, follow the robust stability condition, $\|WPB\|_\infty < 1$. For the amplification limit, a constraint could be added to the optimization process as follows.

$$\left\| (1 - W_1 \frac{A_1}{r_1} e^{-j2\pi f r_1/c} - W_2 \frac{A_2}{r_2} e^{-j2\pi f r_2/c}) \right\|_\infty < 1/D, \tag{12}$$

where $1/D$ is the desired enhancement bound.

Therefore the overall design objective can now be written as:

$$\begin{aligned} &\textbf{\textit{Minimize}} \quad \phi \\ &\textbf{\textit{Subject to}} \\ &\left\| \sqrt{SP_{pb}} S_1 \right\|_\infty < \phi \\ &\left\| \sqrt{SP_{pb}} S_2 \right\|_\infty < \phi \\ &\left\| W_1 B_1 \frac{A_{1o}}{r_{1o}} e^{-j2\pi f r_{1o}/c} + W_2 B_2 \frac{A_{2o}}{r_{2o}} e^{-j2\pi f r_{2o}/c} \right\|_\infty < 1 \\ &\left\| (1 - W_1 \frac{A_1}{r_1} e^{-j2\pi f r_1/c} - W_2 \frac{A_2}{r_2} e^{-j2\pi f r_2/c}) \right\|_\infty < 1/D \end{aligned} \tag{13}$$

where ϕ is a real number, S_1 and S_2 are the sensitivity functions for frequncy range at the left and right half control bandwidth.

It should be noted that constraints on amplification and robust stability will be used in the simulations below. In the next section we will present simulations of $\infty - norm$ pressure minimization over space and frequency.

Results

In this section the simulation results for controlling broad-band diffuse fields using two-channel and three-channel systems are investigated. The primary field is a broad-band diffuse field. Two and three monopoles are used as the secondary fields in the work. A microphone is placed at the (0.1 m, 0) point, i.e., 10cm from the secondary monopole source. A series of simulations are performed to evaluate the performance of an active broad-band noise control. The theory described in previous section is used for the simulations.

In the first example two secondary monopoles are used to control the broad-band disturbance. Eq. 13 was used in the design process. An amplification constraint not exceeding 20dB at the spatial axis from r=0.1m to r=0.2m for all frequencies and a constraint on robust stability with $B_1=B_2=0.3$ were used. The coefficients of the control filters with 64 coefficients were calculated using the function *fmincon()* in MATLAB. The attenuation contour over space and frequency for the two-channel system is shown in Fig. 2. The secondary monopoles are located at the origin and (-0.05 m, 0) point, and the minimization area is the region enclosed in the rectangle as shown in Fig. 2. From the figure we can observe that a high attenuation is achieved in the desired region. It can also be noted that the shape of the high-attenuation area is similar to that of the minimization region. This is because two monopoles could generate complicated secondary fields. Thus a good performance over the minimization region was obtained. A high amplification also appears at high-frequency regions and at the region close to the secondary monopoles.

In the second example three secondary monopoles are used to control the broadband disturbance. The attenuation contour over space and frequency for three-channel system is shown in Fig. 3. A constraint on robust stability for $B_1=B_2=B_3=0.3$ and an amplification constraint not to exceed 20dB at the spatial axis from r=0.1m to r=0.2m for all frequencies were used in the design process. The secondary monopoles are located at the origin, (-0.03m, 0) and (0.03m, 0) points and the minimization region is larger than that in the two-channel system as shown in the figure. From the figure we can see that high attenuation is achieved in the desired region which is larger than that in the two secondary monopole case as shown in Fig. 2. It can also be seen that the shape of the high attenuation area is similar to that of the minimization region. This is because three secondary monopoles created more complicated secondary fields than those in the two secondary monopoles. Thus better performance over the minimization region was obtained as expected. High amplification also appears at high frequencies and at the region close to the secondary monopoles.

In the third example the effect of different minimization shapes on the size of the attenuation contours for three secondary monopoles has also been investigated in this study. Figs. 4 (a) and (b) show the attenuation contours over space and frequency for three secondary monopoles without constraints on robust stability and amplification for different minimization shapes. It can be seen that the shape of the 10dB attenuation contour changes with the minimization shape. In Fig. 4 (a) the 10dB attenuation contour has a narrow shape in frequency axis and longer in space axis similar to the minimization shape. When the minimization shape changes to be narrower in space axis and longer in frequency axis, the 10dB attenuation contour tends to extend its size in the frequency axis as shown in Fig. 4 (b). Therefore the shapes of the 10dB attenuation contour can be designed using the method presented in the paper.

Conclusions

The theory of active control for a broad-band diffuse field using two-channel and three-channel systems has been presented and the performance has been investigated through computer simulations. The acoustic pressure was minimized at the specified region over space and frequency. Constraints on amplification and robust stability were also included in the design process. The results showed that a good attenuation could be achieved at the desired range over space and frequency using a two-channel system. However, a better performance was achieved using a three-channel system. It has also been shown that acoustic pressure could be minimized at a specific frequency range and at a specific location in space away from the microphone. This could be realized by virtual microphone methods. Moreover, the shapes of the 10dB attenuation contour could be controlled using a three-channel system.

Acknowledgment

The study was supported by the National Science Council of Taiwan, the Republic of China, under project number NSC-100-2221-E-018-010.

References

[1] C. F. Ross, ‘‘Active control of sound’’, Dr. Thesis, University of Cambridge, U. K., 1980.

[2] P. Joseph, ‘‘Active control of high frequency enclosed sound fields’’, Dr. Thesis, University of Southampton, U. K., 1990.

[3] B. Rafaely, ‘‘Active control with optimisation over frequency and space’’, *ACTIVE 99*. p.1005, 1999.

[4] Rafaely, B. "Spatial-temporal correlation of a diffuse sound field," *Journal of the Acoustical Society of America*, 107(6), p3254-3258, 2000.

[5] Garcia-Bonito, J, Elliott, S.J. and Boucher, C.C.. ‘‘A novel secondary source for a local active noise control system’’. *ACTIVE 97*, p405-418, 1997.

[6] Jacobsen, F.. ‘‘The diffuse sound field’’. *Report no. 27*, The Acoustics Laboratory, Technical University of Denmark, 1979.

[7] M. Morari, and E. Zafiriou: *Robust Process Control* Prentice-Hall, NJ. 1989.

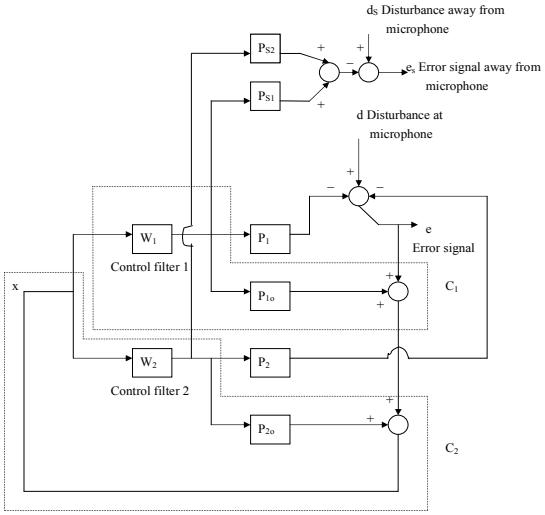

Fig. 1 Two-channel feedback control system with two internal model controllers.

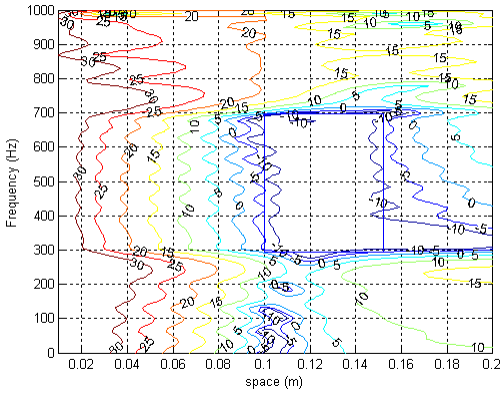

Fig. 2 Attenuation in decibels as function of space and frequency for a two-channel system with two FIR filters having 64 coefficients and with constraints on amplification not exceeding 20dB at spatial axis from r=0.1m to r=0.2m for all frequencies and constraints on robust stability with $B_1 = B_2 = 0.3$.

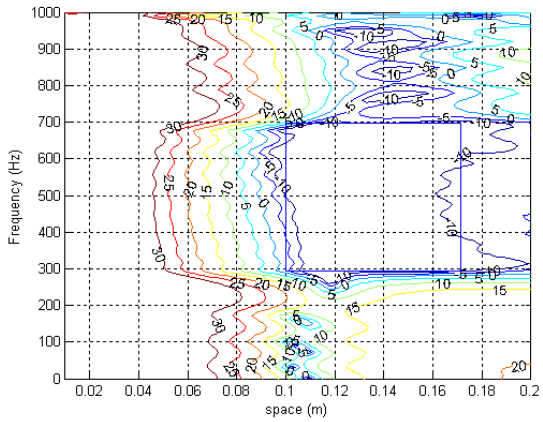

Fig. 3 Attenuation in decibels as a function of space and frequency for a three-channel system with FIR filters having 64 coefficients and constraints on robust stability for $B_1=B_2=B_3=0.3$ and amplification not to exceed 20dB at the spatial axis from r=0.1m to r=0.2m for all the frequencies.

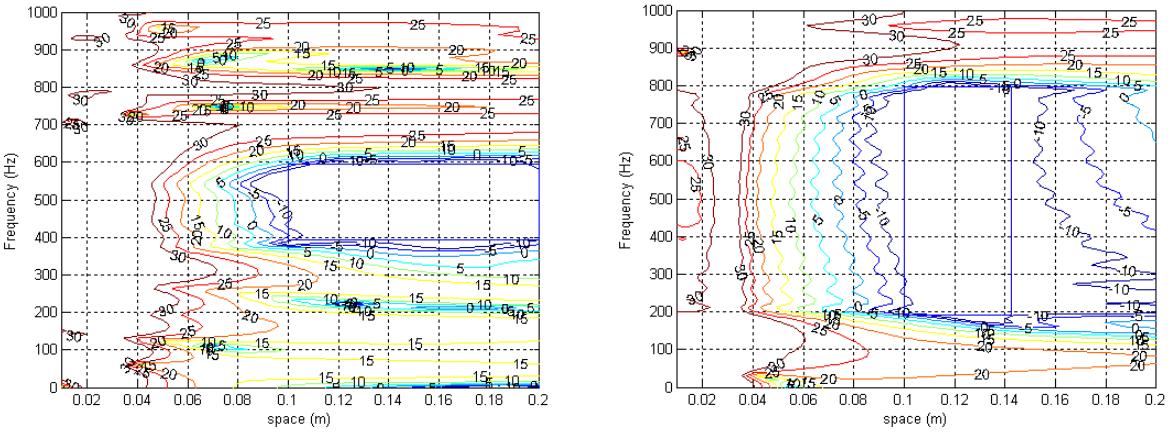

(a) (b)

Figure 4. Attenuation in decibels as a function of space and frequency for a three-channel system with FIR filters having 64 coefficients without constraints for the different minimization shape represented by a bold rectangular frame. (a) The rectangular frame is narrow in the frequency axis direction and longer in the space axis direction. (b) The rectangular frame is narrow in the space axis direction and longer in the frequency axis direction.